SENSITIVITY ANALYSIS IN A LIDAR-CAMERA CALIBRATION

Angel-Iván García-Moreno[1], José-Joel Gonzalez-Barbosa[1], Juan B. Hurtado-Ramos and Francisco-Javier Ornelas-Rodriguez.

[1]Research Center for Applied Science and Advanced Technology (CICATA), Instituto Politécnico Nacional (IPN). Cerro Blanco 141 Col. Colinas del Cimatario, Querétaro, México.
angelivan.garciam@gmail.com

ABSTRACT

In this paper, variability analysis was performed on the model calibration methodology between a multi-camera system and a LiDAR laser sensor (Light Detection and Ranging). Both sensors are used to digitize urban environments. A practical and complete methodology is presented to predict the error propagation inside the LiDAR-camera calibration. We perform a sensitivity analysis in a local and global way. The local approach analyses the output variance with respect to the input, only one parameter is varied at once. In the global sensitivity approach, all parameters are varied simultaneously and sensitivity indexes are calculated on the total variation range of the input parameters. We quantify the uncertainty behaviour in the intrinsic camera parameters and the relationship between the noisy data of both sensors and their calibration. We calculated the sensitivity indexes by two techniques, Sobol and FAST (Fourier amplitude sensitivity test). Statistics of the sensitivity analysis are displayed for each sensor, the sensitivity ratio in laser-camera calibration data

KEYWORDS

Sensitivity analysis, Remote sensing, LIDAR calibration, Camera calibration.

1. INTRODUCTION

Many papers address the calibration LiDAR-camera but very few papers address the uncertainty and sensitivity analysis in the data fusion between a laser sensor and a camera. The interest of this development is to present a study of the quantification of the variability in own methodology results according to the input uncertainties in the calibration model of a multi-sensor platform for urban dimensional reconstruction tasks.

Once the calibration model and data fusion are defined, the sensitivity analysis will determine the uncertainty in input parameters [13]. Many approaches to sensitivity analysis and uncertainty exist, including (1) based on sampling, that uses samples generation considering its probability distribution to analyze the results of its variation [7], (2) differential analysis, which is to approximate the model to a Taylor series and then performing an analysis of variance to obtain the sensitivity analysis [2], (3) Fourier amplitude sensitivity test (FAST), is based on the variation

Jan Zizka et al. (Eds) : ICAITA, SAI, CDKP, Signal, NCO - 2015
pp. 227–239, 2015. © CS & IT-CSCP 2015 DOI : 10.5121/csit.2015.51518

of the predictions of the models and the contributions of individual variables to the variance [14], (4) response surface methodology (RSM) in which an experiment is designed to provide a reasonable response values of the model and then, determine the mathematical model that best fits. The ultimate goal of RSM is to establish the values of the factors that optimize the response (cost, time, efficiency, etc.) [11].

Generally, it can perform a sensitivity analysis in a local or global way [13]. The local approach analyses the output variance with respect to the input parameters. Input parameters are altered within a small range around a nominal value and a particular analysis of each parameter is performed. This analysis only provide information based where it is calculated, since no analyses the entire input parameter space. Furthermore, if the model is not continuous the analysis is unable to be performed. On the other hand, global sensitivity approach defines the uncertainty of the output to the uncertainty of the input factors, by sampling Probability Density Functions (PDF) associated with the input parameters. For this approach, all parameters are varied simultaneously and sensitivity indexes are calculated on the total variation range of the input parameters.

The Monte Carlo (MC) method provides a standard technique for assessing uncertainty in models and modeling data fusion; simulating and sampling the input variables [8,17]. The MC method generates pre-defined pseudo-random numbers with a probability distribution according to its *PDF*. The number of sequences to be simulated must be determined according to the recommendation in [4]. When a model contains too many variables, the uncertainty and sensitivity analysis using Monte Carlo method becomes difficult and with a high computationally cost. This difficulty arises because too many variables require a large number of simulations.

In the Latin Hypercube Sampling (LHS) method, parameters are treated as pseudo-strata and numbers are distributed in proportion to the elements of each strata sample. The *PDF* is generated from the average of each stratum and must have the same distribution of the elements in the sample strata to be calculated under predetermined conditions. The amount of pseudo-random numbers to be generated for the simulation is set similarly to that defined in MC. An analysis of the efficiency and speed of the LHS method against MC method is presented in [01].

Other methods for global sensitivity analysis are presented in [3, 9, 12].

2. MODEL ACQUISITION PLATFORM

The goal is geometrically model our multi-sensors platform behaviour (Fig. 1). Consists by a *Velodyne HDL-64E* laser scanner, a *Point Grey Ladybug2* multi-camera system.

2.1. LiDAR model

To calculate the LiDAR extrinsic parameters, the methodology presented in [5] was implemented. The three-dimensional data is modeled as an $AllPointCloud = f(\boldsymbol{r}, \theta, \phi)$ with respect to origin, where $\boldsymbol{r}$ is the radius of the surface, θ colatitude or zenith angle, and ϕ azimuthal angle on the unit sphere. The development of the mathematical model for the captured 3D points is based on the transformation of the spherical coordinates for each position of the unitary sphere onto cartesian coordinates. The key point of this transformation is that every involved parameter includes a perturbation as defined in Eq. 1.

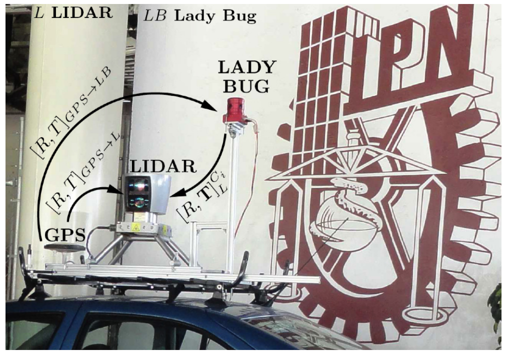

Figure 1 Sensor platform composed of LiDAR Velodyne HDL-64E (*L*), *Ladybug2* (*LB*) and GPS. *Ladybug* spherical digital video camera system has six cameras (*C*). $[\mathbf{R},\mathbf{T}]_{\mathbf{L}}^{\mathbf{C}}$ represent translation and rotation of the LiDAR and six camera frames of the *Ladybug2*.

$$\begin{aligned} x' &= d_x' \sin(\theta + \Delta\theta) - h_{OSC} \cos(\theta + \Delta\theta), \\ y' &= d_x' \cos(\theta + \Delta\theta) + h_{OSC} \sin(\theta + \Delta\theta), \\ z' &= (ds + \Delta ds)\sin(\phi + \Delta\phi) + v_{OSC} \cos(\phi + \Delta\phi), \end{aligned} \tag{1}$$

where $d_x' = (ds + \Delta d_s)\cos(\phi + \Delta\phi) - v_{OSC}\sin\phi + \Delta\phi$, see Fig. 2.

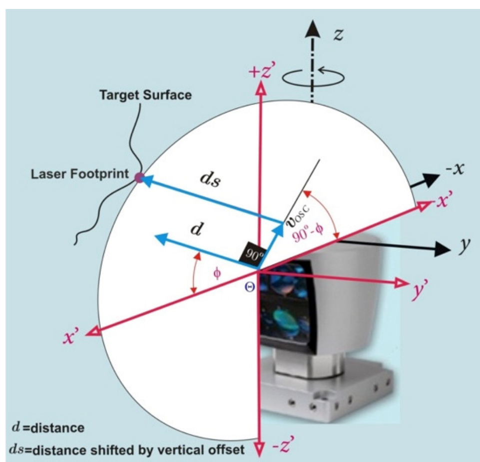

Figure 2 LiDAR Velodyne HDL-64E configuration.

2.2. Multi-camera model

To get the intrinsic parameters we followed the calibration methodology presented in [18]. A camera is modeled by the usual pinhole camera model: The image $\boldsymbol{u}^C$ of a 3D point $\boldsymbol{X}^L$ is formed by an optical ray from $\boldsymbol{X}^L$ passing through the optical center *C* and intersecting the image plane. The relationship between the 3D point $\boldsymbol{X}^L$ and its image projection $\boldsymbol{u}^C$ is given by Eq. 2.

$$s\hat{u}^C = A^C[R_L^C, T_L^C]\hat{\boldsymbol{X}}^L = P_L^C\hat{\boldsymbol{X}}^L \tag{2}$$

with $A^C = \begin{bmatrix} -k_u f & 0 & u_0 & 0 \\ 0 & k_v f & v_0 & 0 \\ 0 & 0 & 1 & 0 \end{bmatrix}$

and $A^C[R_L^C, \boldsymbol{T}_L^C]$,

where s is a scale factor, $[R_L^C, \boldsymbol{T}_L^C]$ are the extrinsic parameters and represent the rigid transformation between a point in the LiDAR frame L to the camera frame C, A^C is the intrinsic camera parameters matrix, where (u_o, v_0) are the principal point coordinates in the image, focal length f, $-k_u f = \alpha \; and \; k_v f = \beta$ are the image scale factors in the axis u y v. The P_L^C is the projection matrix.

2.3. LiDAR-camera calibration

The extrinsic transformation between the LiDAR and the camera frame was computed using Eq. 3.

$$[R_L^C, \boldsymbol{T}_L^C] = [R_L^C, \boldsymbol{T}_L^C]_W^C * \; ([R, \boldsymbol{T}]_W^L)^{-1} \tag{3}$$

where R and $\boldsymbol{T}$ represents de rotation and translation respectively, C and L are the camera and LiDAR and W represents the word frame.

The pattern acquired by the LiDAR is transformed onto the image frame using the extrinsic parameters $[R_L^{C_i}, \boldsymbol{T}_L^{C_i}]$. This transformation allows us to reference in the camera the points acquired by the LiDAR. The projection is completed using the intrinsic camera parameters A^C, Fig. 3.

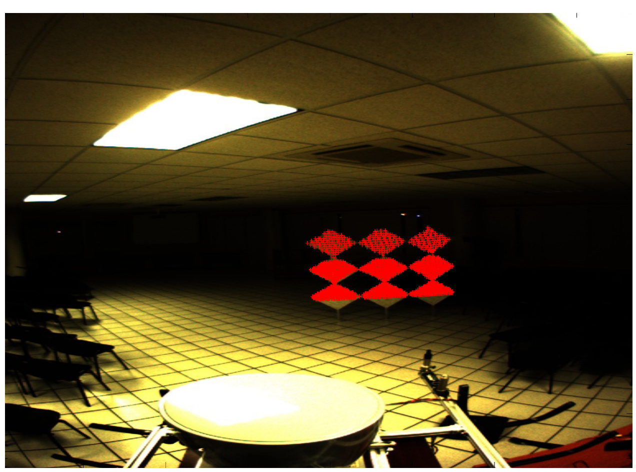

Figure 3 The red points are acquired by the LiDAR and projected onto the image.

3. SENSITIVITY ANALYSIS

Two techniques were used for analysis, Sobol and FAST. The advantages that are: (1) parameters are evaluated throughout its range of variation, (2) estimating the expected values and the variance of each parameter is calculated directly, (3) calculate the contribution that each parameter has on the global sensitivity, (4) determine the effects of the interaction between the parameters in the sensitivity analysis, and (5) no modifications are required in the calibration model for the analysis.

3.1. Sobol

Suppose the model is given by $Y = f(X_1, X_2, \dots, X_k)$, where X_i are independent input parameters, Y is the model output. Using dispersion analysis by [1], f can be linear or nonlinear, and the sensitivity analysis evaluates the contribution of each parameter X_i in the variance of Y. This study is known as analysis of variance (ANOVA). For sensitivity indices for each parameter independently V variance model is decomposed as:

$$\mathrm{V} = \sum_{\mathrm{i}} \mathrm{V_i} + \sum_{\mathrm{i}<j} V_{i,j} + \sum_{\mathrm{i}<j<m} V_{i,j,m} + \cdots + \mathrm{V_k} \tag{4}$$

where $V_k = V\left(E\left(Y \middle| X_i, X_j, \dots, X_k\right)\right) - V_i - V_j - \cdots - V_k$. As a rule, the Eq. 4 has a total of terms $\sum\left(C_1^k + C_2^2 + \cdots + C_k^k\right) = 2^k - 1$. Sensitivity analysis indices are computed:

$$\mathrm{S}_{\mathrm{i}_1, i_2, \dots, i_k} = \frac{\mathrm{V}_{\mathrm{i}_1, i_2, \dots, i_k}}{\mathrm{V}} \tag{5}$$

where $i_1, i_2, \cdots, i_k$ are the input parameters. Then, all the sensitivity indexes that allow us to observe the interaction between inputs and nonlinearity must meet the condition:

$$\sum_{\mathrm{i}=1}^{\mathrm{k}} S_i + \sum_{i} \sum_{j>i} S_{i,j} + \cdots + S_k = 1 \tag{6}$$

On the other hand, the index $S_i = \frac{V_i}{V}$ only shows the effect of the parameter X_i in the model output, but not analyzes the interaction with other parameters. To estimate the total influence of each parameter, the total partial variance is calculated:

$$V_i^{tot} = \sum_{\mathrm{i}} V_{i_1, \dots, i_k} \tag{7}$$

the sum is over all the different groups of indexes that satisfy the condition $1 \leq i_1 < i_2 < \cdots < i_k \leq s$, where one of the indexes is equal to *i*. Then, the total sensitivity index is given by:

$$S_i^{tot} = \frac{\mathrm{V_i^{tot}}}{V} \tag{8}$$

The total sensitivity index (total variance) S_i^{tot} represents the expected percentage of the variance that remains in the model output if all the parameters are known except *i*. It follows then $0 \leq S_i \leq S_i^{tot} \leq 1$. The result is S_i^{tot} and S_i indicates the interaction between parameter *i* and the other ones.

3.2. FAST

FAST allows generate independent sensitivity indexes for each input parameter using the same number of iterations. The method idea is convert Eq. 4 in a uni-dimensional integer s using the transformation functions G_i:

$$X_i = G_i(\sin \omega_i s) \tag{9}$$

where $s \in (-\pi, \pi)$. A good choice of the transformation G_i and frequency ω_i will assess the model in a sufficient number of points [14]. Then the expected value of Y can be approximated by:

$$E(Y) = \frac{1}{2\pi}\int_{-\pi}^{\pi} f(s)ds \tag{10}$$

by

$$f(s) = f(G_1(\sin \omega_1 s), \dots, G_k(\sin \omega_k s)) \tag{11}$$

So therefore, we can approximate the variance of Y as:

$$\begin{aligned} V(Y) &= \frac{1}{2\pi}\int_{-\pi}^{\pi} f^2(s)ds - [E(Y)]^2 \\ &\approx \sum_{i=-\infty}^{\infty} \left(A_i^2 + B_i^2\right) - (A_0^2 + B_0^2) \\ &\approx 2\sum_{i=1}^{\infty} \left(A_i^2 + B_i^2\right) \end{aligned} \tag{12}$$

where A_i and B_i are the Fourier coefficients. The contribution of X_i in the variance $V(Y)$ can be approximated by:

$$D_i \approx \sum_{p=1}^{M} (A_{p\omega i}^2 + B_{p\omega i}^2) \tag{13}$$

where ωi is related to the value G_i in Eq. 11 by $p = 1,2 \cdots M$. Will then M, the maximum harmonic. The sensitivity coefficients by the FAST method for each parameter is calculated:

$$S_i = \frac{\mathrm{V_i}}{V(Y)} \doteq \frac{\sum_{p=1}^{M}(A_{p\omega i}^2 + B_{p\omega i}^2)}{\sum_{i=1}^{M}\left(A_i^2 + B_i^2\right)} \tag{14}$$

4. RESULTS

4.1. Sensitivity

4.1.1. Ladybug2

Were simulated *2,000* samples by MC and LHS. The camera was intrinsically calibrated by the method presented in [18]. Sobol was the first technique in which the camera sensitivity was assessed (section 3.1). The determination of global indexes (S_i) and total indexes (S_i^{tot}) according to equations 5 and 8 respectively, requires high computational consumption due to the high number of operations performed to decompose the variance of the model for each parameters and the correlation between them. Fig. 4 shows six graphs, one for each distribution on which the sensitivity analysis was performed. It has to be emphasized that the Sobol sequence [15] (which generates random numbers with low discrepancy) is totally different to the Sobol method for calculating the sensitivity indexes described in section 3.1.

Zhang's method shows that the parameter with greater global sensitivity is *tz*. Furthermore, also the parameter with greater total sensitivity is β. A similar behavior but analyzed from the error propagation perspective in LiDAR-camera calibration is presented in [6]. We can define that the parameters involved directly with the distance of the calibration pattern and image distortions tend to be the most relevant in the error propagation in our calibration system. This error can be minimized in two ways: (1) removing the image distortion and standardizing the images and (2) increasing the reference points in the calibration process. Furthermore, this demonstrates the flexibility to use a calibration approach using a pattern plane.

The second technique implemented for sensitivity analysis of the camera was FAST. This technique gives us the first order indexes S_i by Eq. 14. Table I shows the sensitivity quantified by FAST. It is noted that the parameter *tz* is the more sensitive one. Just as the Sobol method, depth is important. Using a pattern with more corners can reduce this condition. These results confirm experiments made empirically by [16] and also the behaviour shown in Figure 4.

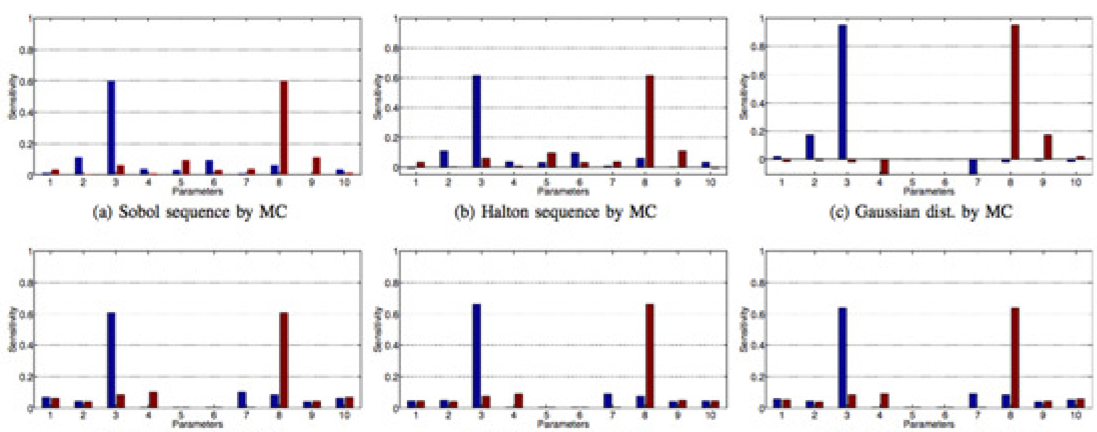

(a) Sobol sequence by MC (b) Halton sequence by MC (c) Gaussian dist. by MC

(d) Gaussian dist. by LHS (e) Uniform dist. by LHS (f) Multivariate dist. by LHS

Figure 3 Zhang's calibration method analyzed by Sobol technique, blue bars are the global sensitivity ($\boldsymbol{S_i}$) and red bars are the total sensitivity $\boldsymbol{S_i^{tot}}$**.** Simulated data by MC and LHS with six different distributions. The most relevant parameters are *tz* and $\boldsymbol{\beta}$, i.e. with more sensitive. Table I shows the number parameters reference.

Table 1 Sensitivity analysis by FAST method according to Eq. 14. It is noted that tz and ty parameters are the most sensitive. Only tz parameter agrees with the analysis by the Sobol method, marking a tendency to introduce error in the camera calibration.

Reference	*Parameter*	*Sensitivity index*
1	*tx*	0.0130
2	*ty*	0.1108
3	*tz*	0.5998
4	*wx*	0.0380
5	*wy*	0.0329
6	*wz*	0.0960
7	α	0.0081
8	β	0.0619
9	*u0*	0.0031
10	*v0*	0.0363

4.1.2. LiDAR

The LiDAR sensitivity indexes by Sobol method was calculated as the camera. Figure 5 shows the global (S_i) and total (S_i^{tot}) indexes. It can be seen, that the parameters θ and $\Delta\theta$ are introducing greater uncertainty in the calibration model. The θ parameter corresponds to the LiDAR orientation angle, and is related to the mechanical rotation, while $\Delta\theta$ is a correction of the orientation of each LiDAR laser, because not all of them are in a single plane. Variations in θ and $\Delta\theta$ parameters induce measurement errors because the LiDAR is oriented at a single plane, when actually LiDAR lasers are register a near plane.

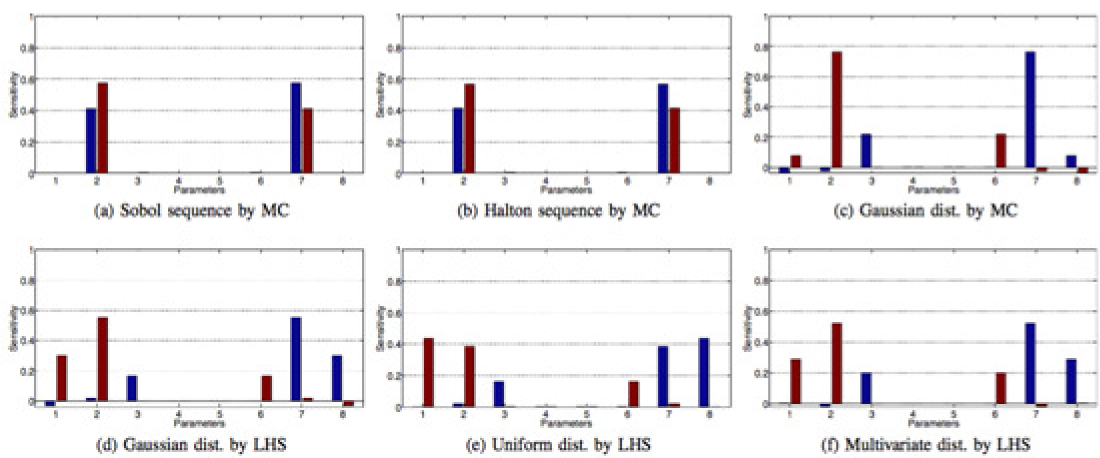

Figure 4 LiDAR sensitivity analysis by Sobol method, blue bars are the global sensitivity($\boldsymbol{S_i}$) and red bars are the total sensitivity ($\boldsymbol{S_i^{tot}}$). Simulated data by MC and LHS with six different distributions. The most relevant parameters are $\boldsymbol{\theta}$ and $\boldsymbol{\Delta\theta}$, i.e. with more sensitive. Table II shows the number parameters reference

Through the FAST technique, sensitivity indexes match to Sobol technique as shown in Table II. The θ and $\Delta\theta$ are the most sensitive parameters and introducing more noise in the model, and hence increase the output uncertainty error in the calibration values.

Table 2 Sensitivity analysis by FAST technique according to equation 14. It is noted that $\boldsymbol{\theta}$ and $\boldsymbol{\Delta\theta}$ parameters are the most sensitive to introduce error into the laser sensor calibration.

Reference	*Parameter*	*Sensitivity index*
1	ds	0.0140
2	θ	0.4137
3	ϕ	0.0004
4	V_{osc}	0.0160
5	H_{osc}	0.000
6	Δds	0.0006
7	$\Delta\theta$	0.5552
8	$\Delta\phi$	0.000

4.2. Uncertainty

4.2.1. Ladybug2

The uncertainty analysis was conducted to determine the nominal values of the model's error, according to the preliminary sensitivity analysis. Results obtained from a LHS simulation are shown in Table III in which we computed the extrinsic parameters $[R,\boldsymbol{T}]_{\mathrm{W}}^{\mathrm{C}}$ and the intrinsic parameters, image center (u_0, v_0), focal length (α, β).

Table 3 Extrinsic-intrinsic uncertainty camera parameters

	Mean	*Std*
Translation (mm) $\begin{bmatrix} tx \\ ty \\ tz \end{bmatrix}$	$\begin{bmatrix} -125.82 \\ -21.50 \\ 339.43 \end{bmatrix}$	$\begin{bmatrix} 0.0012 \\ 0.0017 \\ 0.0075 \end{bmatrix}$
Rotation (rad) $\begin{bmatrix} roll \\ pitch \\ yaw \end{bmatrix}$	$\begin{bmatrix} -2.22 \\ -2.14 \\ -2.13 \end{bmatrix}$	$\begin{bmatrix} 3.88 \\ 4.37 \\ 4.44 \end{bmatrix} \times 10^{-6}$
Focal (mm)	(551,34,550.81)	(0.0013,0.0014)
Image center (px)	(388.61,506.62)	(0.0025, 0.0029)

Fig. 6 shows graphics simulated uncertainty calculation. Both series of intrinsic and extrinsic parameters exhibit a linear behaviour. Uncertainties were obtained when normal distribution $N(0,\sigma)$ Gaussian noise was added to feature points extracted from the pattern(corners). σ parameter was the result of projecting real-world pattern feature point coordinates' on image plane, its value was 10 pixels. Average error for our projection algorithm was then calculated by measuring the differences between extracted feature points of the whole set of images and those of the real pattern, this error was calculated to a value of *0.25* pixels. Figure 6(a) shows the *Z* axis error tends to increase more than the other axes. Figure 6(c) shows that the error is stable and incremental for both axes while noise increases.

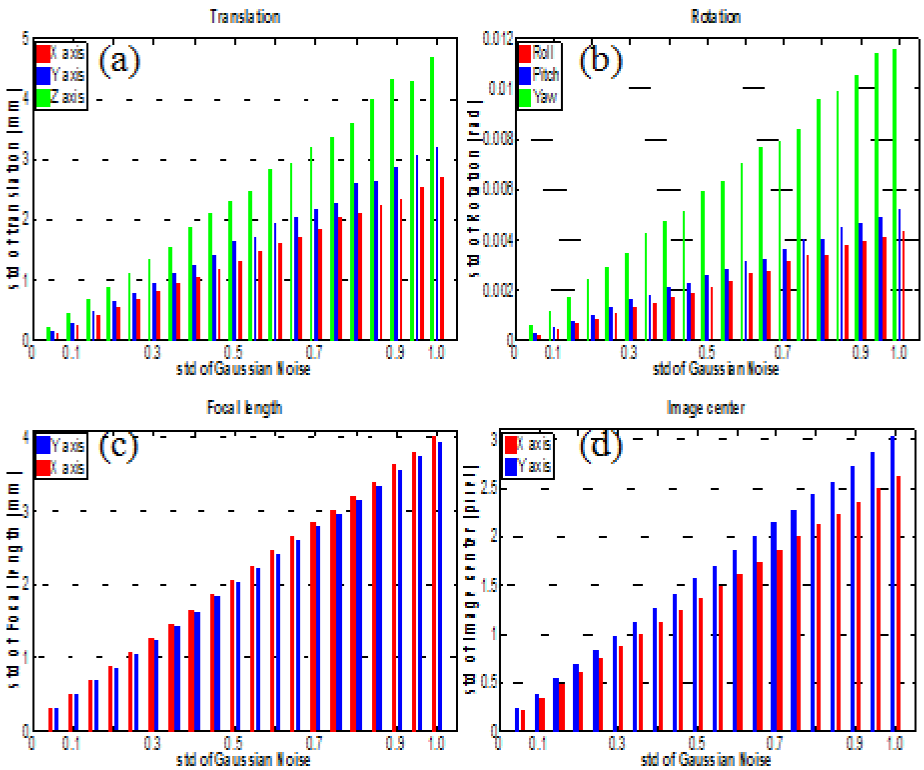

Figure 5 Simulated camera parameters performance. Ordinate axis represents the standard deviation of *2,000* iterations using LHS simulation.

4.2.2. LiDAR

Table IV shows the uncertainty on extrinsic parameters with respect to the world frame. Using a LHS simulation, noise was added to the feature points to evaluate the behaviour of error in these two parameters.

Table 4 Uncertainty on extrinsic LiDAR parameters $[\boldsymbol{R},\boldsymbol{T}]_{\mathrm{W}}^{\mathrm{L}}$

	Mean	*Std*
Translation (mm) $\begin{bmatrix} tx \\ ty \\ tz \end{bmatrix}$	$\begin{bmatrix} -515.29 \\ 165.62 \\ -39.06 \end{bmatrix}$	$\begin{bmatrix} -1.58 \\ 1.08 \\ -1.92 \end{bmatrix}$
Rotation (rad) $\begin{bmatrix} roll \\ pitch \\ yaw \end{bmatrix}$	$\begin{bmatrix} 0.55 \\ 1.51 \\ 1.52 \end{bmatrix}$	$\begin{bmatrix} 0.015 \\ 0.011 \\ 0.012 \end{bmatrix}$

4. CONCLUSIONS

Variability analysis in the LiDAR-camera calibration is compute. We estimate the relationship between the input and the output quantity in a implicit form. The sensitivity of the calibration depends on the measurements quality, the model used, the calibration method and the conditions under which it is performed. A sensitivity analysis was performed on models of individual calibration of a multi-camera system and a laser sensor. Two techniques are presented for this analysis. Sobol technique, which is based on the decomposition analysis of the variance for each input parameter into the model. And the FAST technique, which uses a Fourier series to represent a multivariable function in the frequency domain using a single variable frequency. For each one of these techniques, we simulated data by two methods: (1) Monte Carlo method and (2) Latin Hypercube sampling method. Since each parameter in the calibration has its own probability distribution, and wanting to generalize the sensitivity analysis, the data were simulated with 6 different types of distributions to cover a higher outlook in this analysis.

It was shown that the parameters tz and β are the most sensitive in the calibration camera model. Sensitivity tests for the calibration method presented in [18] were performed. It was concluded that the parameters involved in the distance between the camera and the calibration pattern (depth) are the most likely to introduce error in the final values of camera calibration, as also concluded in uncertainty analysis in [6] Now that the system behaviour is known, we can pay more attention to characterize the uncertainty in these parameters. LHS method tends to calculate more stable results, i.e. with less variability. On the other hand, it is true that Sobol and FAST techniques allows an extensive sensitivity analysis. The downside is while more parameters the model has more computation time is required to decompose the variance. In our case, the more suitable methodology to simulate data to perform a sensitivity analysis is LHS. In the LiDAR calibration, the parameters θ and $\Delta\theta$ are introducing greater uncertainty in the calibration model. The θ parameter corresponds to the LiDAR orientation angle, and is related to the mechanical rotation, while $\Delta\theta$ is a correction of the orientation of each LiDAR laser. Variations in θ and $\Delta\theta$ parameters induce measurement errors because the LiDAR is oriented at a single plane, when actually LiDAR lasers are registering a near plane.

On the other hand, the uncertainty analysis shows a deviation as small as *0.003 mm* on the translation vector it has been shown that the proposed calibration method is robust and reliable a very small rotation deviation in the order of micro radians has also been obtained. These results contribute to a high level of measurement confidence, despite the complicated working conditions in which our platforms is used. One can now rely on maintaining an acceptable error propagation and uncertainty range in future data fusion operations and 3D texturization. Capture platform has been designed to digitize urban environments, which are mainly a set of planes. For a plane reconstruction (e.g. front of a house) located at 4 meters or less from the system we found a reconstruction error of *2 cm*.

In future works, using some other calibration methods, we expect to be able to minimize this error propagation and uncertainty. Mainly by using data from different calibration instruments. At the end we will be able of compensating the error in 3D reconstruction.

REFERENCES

[1] GEB Archer, A. Saltelli, and IM Sobol. Sensitivity measures, anova-like techniques and the use of bootstrap. Journal of Statistical Computation and Simulation, 58(2):99–120, 1997.

[2] Dan G Cacuci, Mihaela Ionescu-Bujor, and Ionel Michael Navon. Sensitivity and Uncertainty Analysis: Applications to large-scale systems, volume 2. CRC Press, 2004.

[3] Roger A Cropp and Roger D Braddock. The new morris method: An efficient second-order screening method. Reliability Engineering & System Safety, 78(1):77–83, 2002.

[4] Arnaud Doucet, Simon Godsill, and Christophe Andrieu. On sequential monte carlo sampling methods for bayesian filtering. Statistics and computing, 10(3):197–208, 2000.

[5] Angel-Iván García-Moreno, José-JoelGonzalez-Barbosa, Francisco-Javier Ornelas-Rodriguez, Juan B Hurtado-Ramos, and Marco-Neri Primo-Fuentes. Lidar and panoramic camera extrinsic calibration approach using a pattern plane. In Pattern Recognition. Springer, 2013.

[6] Angel-Iván García-Moreno, Denis-Eduardo Hernandez-García, José-Joel Gonzalez-Barbosa, Alfonso Ramírez-Pedraza, Juan B Hurtado-Ramos, and Francisco-Javier Ornelas-Rodriguez. Error propagation and uncertainty analysis between 3d laser scanner and camera. Robotics and Autonomous Systems, 62(6):782–793, 2014.

[7] J.C. Helton, F.J. Davis, and J.D. Johnson. A comparison of uncertainty and sensitivity analysis results obtained with random and latin hypercube sampling. Reliability Engineering and System Safety, 89(3):305–330, 2005.

[8] L. Lilburne and S. Tarantola. Sensitivity analysis of spatial models. International Journal of Geographical Information Science, 23(2):151–168, 2009.

[9] Hervé Monod, Cédric Naud, and David Makowski. Uncertainty and sensitivity analysis for crop models. D. WALLACH, D. MAKOWSKI et J. JONES, éditeurs: Working with Dynamic Crop Models, pages 55–100, 2006.

[10] Gustavo G Pilger, Joao Felipe CL Costa, and Jair C Koppe. Improving the efficiency of the sequential simulation algorithm using latin hypercube sampling. In Geostatistics Banff 2004. Springer, 2005.

[11] Myers RH. Response surface methodology – current status and future directions. J Qual Technol, 31(1):30–44, 1999.

[12] Andrea Saltelli, Paola Annoni, Ivano Azzini, Francesca Campolongo, Marco Ratto, and Stefano Tarantola. Variance based sensitivity analysis of model output. design and estimator for the total sensitivity index. Computer Physics Communications, 181(2):259–270, 2010.

[13] Andrea Saltelli, Karen Chan, E Marian Scott, et al. Sensitivity analysis. Wiley New York, 2000.

[14] Andrea Saltelli, Stefano Tarantola, Francesca Campolongo, and Marco Ratto. Sensitivity analysis in practice: a guide to assessing scientific models. John Wiley & Sons, 2004.

[15] I.M Sobol'. On the distribution of points in a cube and the approximate evaluation of integrals. {USSR} Computational Mathematics and Mathematical Physics, 7(4):86–112, 1967.

[16] Wei Sun and Jeremy R Cooperstock. An empirical evaluation of factors influencing camera calibration accuracy using three publicly available techniques. Machine Vision and Applications, 17(1):51–67, 2006. [17]Stefan J Wijnholds and A-J Van Der Veen. Multisource self-calibration for sensor arrays. Signal Processing, IEEE Transactions on, 57(9):3512–3522, 2009.

[18] Z. Zhang. A flexible new technique for camera calibration. In IEEE Transactions on Pattern Analysis and Machine Intelligence, pages 1330–1334, 2000.

AUTHORS

Ángel Iván García Moreno. He is currently Ph.D. candidate in Advanced technology from the Research Center for Applied Science and Advanced Technology. He obtained his M.Sc. degree from the National Polytechnic Institute, in 2012, in the computer vision area. He received the B.S. degree in Informatics by the Autonomous University of Queretaro in 2009. His personal interests are computer vision, remote

José Joel González Barbosa was born in Guanajuato, Mexico, in 1974. He received the M.S. degree in Electrical Engineering from the University of Guanajuato, Mexico, and Ph.D. degree in Computer Science and Telecommunications from National Polytechnic Institute of Toulouse, France, in 1998 and 2004, respectively. He is an Associate Professor at the CICATA Querétaro-IPN, Mexico, where he teaches courses in Computer Vision, Image Processing and Pattern Classification. His current research interests include perception and mobile robotics.

Juan B. Hurtado Ramos. He received the B.S. degree in Communications and Electronics Engineering in 1989 by the Guadalajara University. He obtained his Ph.D. degree from the Optics Research Center of the University of Guanajuato in 1999. He is currently a Profesor-Researcher of the CICATA Querétaro-IPN, Mexico in the Image Analysis group. His personal interests are mainly in the field of Metrology using optical techniques. Since 1998, he is member of the Mexican National Researchers System.

Francisco Javier Ornelas Rodriguez. He received the B.S. degree in Electronic Engineering in 1993 by University of Guanajuato. He obtained his Ph.D. degree from the Optics Research Center in 1999. He is currently a Profesor-Researcher of CICATA Querétaro-IPN, Mexico in the Image Analysis team. His personal interests are mainly in the field of Metrology using optical techniques. He is member of the Mexican National Researchers System.